Electric dipole moment function and line intensities for the ground state of carbon monxide*

Chen Hua-Jun(陈华君)[a], Wu Jie(吴 杰)[b], Liu Hao(刘 浩)[b], and Cheng Xin-Lu(程新路)[a]†

[a] *Institute of Atomic and Molecular Physics, Sichuan University, Chengdu* 610065, *China*
[b] *Science and Technology on Optical Radiation Laboratory, Beijing* 100854, *China*

(Received 28 November 2014; revised manuscript received 22 March 2015; published online 20 June 2015)

An accurate electric dipole moment function (EDMF) is obtained for the carbon monoxide (CO) molecule ($X^1\Sigma^+$) by fitting the experimental rovibrational transitional moments. Additionally, an accurate *ab initio* EDMF is found using the highly accurate, multi-reference averaged coupled-pair functional (ACPF) approach with the basis set, aug-cc-pV6Z, and a finite-field with ±0.005 a.u. (The unit a.u. is the abbreviation of atomic unit). This *ab initio* EDMF is very consistent with the fitted ones. The vibrational transition matrix moments and the Herman–Wallis factors, calculated with the Rydberg–Klein–Rees (RKR) potential and the fitted and *ab initio* EDMFs, are compared with experimental measurements. The consistency of these line intensities with the high-resolution transmission (HITRAN) molecular database demonstrates the improved accuracy of the fitted and *ab initio* EDMFs derived in this work.

Keywords: electric dipole moment, vibrational transition matrix moments, Herman–Wallis factors, line intensities

PACS: 31.15.A–, 31.50.Bc, 33.20.Ea, 33.20.Vq **DOI:** 10.1088/1674-1056/24/8/083102

1. Introduction

Carbon monoxide (CO) is a stable and important diatomic molecule and has been detected in interstellar clouds as well as the Earth's atmosphere.[1] The spectral parameters of CO are included in well-known spectroscopic databases such as the high-resolution transmission (HITRAN) molecular database,[2] the high-temperature version of HITRAN called the HITEMP database,[3] and others. For CO and other molecules, calculations of line parameters are closely related to their electric dipole moment functions (EDMFs). With the progress of experimental technology, further investigation of the EDMF for CO ($X^1\Sigma^+$) based on new experimental data is possible.

Several band systems of CO have been observed. Numerous spectral line parameter measurements of CO have been collected for the fundamental band 1–0,[4–7] the first overtone 2–0,[7–11] and the second overtone 3–0.[8,12–17] Many studies in the past decade have focused on the 3–0 band by using a variety of experimental designs. Chackerian and Valero[18] measured the absolute rovibrational intensities of the 4–0 band of carbon monoxide, and more recently Ogilvie *et al.*[19] have evaluated the electric dipolar moments based on new experimental measurements of line strengths including the 4–0 band of $^{12}C^{16}O$. Furthermore, Chung *et al.*[20] adapted a cavity ring-down spectral technique in the near-infrared region to measure the 5–0 band for the first time.

Several EDMFs for the ground state of CO have been deduced with various methods based on experimental data with $\Delta\upsilon \leq 4$.[8,12,19,21–26] For instance, based on the inversion of experimental intensity information, Chackerian and Tipping[22] derived a hybrid EDMF in a Padé approximant. It was used to calculate the rovibrational intensities of the ground state CO ($X^1\Sigma^+$) by Goorvitch *et al.*[27–29] In consideration of these pure vibrational matrix elements of the bands υ'–0 with $0 \leq \upsilon' \leq 5$, Chung *et al.* derived an EDMF in a polynomial form.[20] A considerable number of quantum chemical calculations of EDMFs for CO have been presented in various papers.[19,30–37] However, we find that the vibrational transition matrix elements (or rotationless transition matrix elements) calculated using the quantum chemical EDMFs along with the Rydberg–Klein–Rees (RKR) potential, or *ab initio* potential, actually disagree with the experimental results. Therefore, more accurate theoretical calculations are needed.

In this work, we adopt a direct fit approach to determine an EDMF for the CO $X^1\Sigma^+$ state by utilizing individual, high-quality measurements for line intensities including the 5–0 band. We also perform a series of theoretical calculations to determine the EDMF of the electronic state of CO ($X^1\Sigma^+$). Based on the RKR potential, the eigenfunctions, $\Psi_{\upsilon,J}(r)$, are determined by solving the radial Schrödinger equation of nuclear motion. Eigenfunctions, $\Psi_{\upsilon,J}(r)$, and EDMFs are used to determine the vibrational matrix elements and the Herman–Wallis factors for several bands of CO ($X^1\Sigma^+$). Finally, we calculate the rovibrational line intensities of some bands of CO ($X^1\Sigma^+$) by using the present fitted and *ab initio* EDMFs

*Project supported by the National Natural Science Foundation of China (Grant Nos. 11374217 and 11474207).
†Corresponding author. E-mail: chengxl@scu.edu.cn
© 2015 Chinese Physical Society and IOP Publishing Ltd

and compare them with the published experimental data.

2. Theoretical basis

2.1. Fitted EDMF method

The method of obtaining the EDMF experimentally, as developed by Tipping and Herman, is to assume a power series expansion

$$M(x) = \sum_{i=0} M_i x^i, \tag{1}$$

and to fit the coefficient, M_i, to the measured rotationless transition matrix elements $\langle \upsilon', 0|M(r)|\upsilon'', 0\rangle$.[38] The single and double primes correspond to the upper and lower states, respectively. In Eq. (1), $x = (r - r_e)/r_e$, where r_e is the equilibrium separation and M_0 represents the permanent dipole moment at the minimum potential where $r = r_e$. In a harmonic potential, $M_1 x$ is related to the $\Delta\upsilon = 1$ transitions, while $M_1 x^2$ is related to the $\Delta\upsilon = 2$ transitions and so on.

Using Eq. (1), the rovibrational matrix elements can be written as

$$\left\langle \upsilon', J' \left| M(r) \right| \upsilon'', J'' \right\rangle = \sum_{i=1}^{n} M_i \left\langle \upsilon', J' \left| x^i \right| \upsilon'', J'' \right\rangle. \tag{2}$$

Thus, the inclusion of rotational components allows a better determination of the M_i coefficients by fitting to a greater number of points.[39,40] In order to derive the new EDMF from Eq. (2), we identify the best available experimental results for each band. We use the results of Zou *et al.*[7] for the fundamental band, Brulat *et al.*'s[41] for the first overtone band, Sung *et al.*'s[17] for the 3–0 band, Chackerian *et al.*'s[18] for the 4–0 band, and Chung *et al.*'s[20] for the 5–0 band. Moreover, in order to obtain the accurate coefficient M_0, the value of the matrix moment $\mu_{\upsilon'=0,\upsilon''=0} = 0.10982$ Debye as reported by Chackerian *et al.*[6] is also included in the fitting work. The weighted and unweighted fits of all data are performed.

2.2. Theoretical computational details

The ground state carbon monoxide molecule is a closed-shell molecule, and the electric configuration of the CO $X^1\Sigma^+$ is $1\sigma^2 2\sigma^2 3\sigma^2 4\sigma^2 1\pi_x^2 1\pi_y^2 5\sigma^2$, which has a_1 symmetry. We compute the EDMF by using highly correlated *ab initio* methods, namely, the complete active space self-consistent field (CASSCF)[42] approach followed by the highly accurate averaged coupled-pair functional (ACPF)[43] method in the C_{2V} point group.

The EDMF calculations are performed by using the MOLPRO 2009.1 program package,[44] with and without a finite-field approach with field values of ± 0.005 a.u. We separately use the aug-cc-pV6Z (aV6Z) and spdfghi aug-cc-pV6Z (spdfghi aV6Z) basis sets of Dunning *et al.* for both C and O atoms.[45–47] These basis sets are sufficiently diffuse to describe long-range interactions so that a more accurate EDMF can be determined at larger internuclear separations. In this work, we only consider the electric correlation energy of valence electrons and only choose the full valence active spaces consisting of eight valence orbitals, which is denoted by (4220) in C_{2V} point group symmetry.

With the aid of Le Roy's LEVEL 8.0 program,[48] the piecewise polynomial interpolation is performed by using numerical input potential energies and electric dipole moments. The rovibrational matrix elements are obtained through the use of the fitted EDMF and the theoretically calculated EDMF, together with an RKR potential energy function. The RKR potential curves for CO are constructed by using the purely numerical RKR method with Dunham coefficients from Velichko *et al.* who provided accurate molecular parameters for higher-lying vibrational levels (up to $\upsilon = 41$).[49,50]

3. Results and discussion

3.1. Details of calculations and results

The RKR potential is employed to calculate the transition wavenumbers, lower-state energies, and the expectation values $\langle \upsilon', J'|x^i|0, J''\rangle$ by using Le Roy's LEVEL 8.0 program.[48] The rovibrational matrix elements are then evaluated from the measured line intensities according to

$$\begin{aligned} S \;=\; & (8\pi^3/3hc)[\exp(-hcE_{0J}/k_BT)/4\pi\varepsilon_0 Q(T)] \\ & \times \sigma_0[1-\exp(-hc\sigma_0/k_BT)]\,|m| \\ & \times \left|\langle \upsilon' J' \left| M(x) \right| \upsilon'' J'' \rangle\right|^2, \end{aligned} \tag{3}$$

where S is the line intensity for pure $^{12}C^{16}O$ in cm^{-1}/mol; h, c, and k are Planck constant, velocity of light, and Boltzmann constant, respectively; σ_0 is the transition wavenumber in cm^{-1}; T is the temperature; $Q(T)$ is the total internal partition; $m = 1/2[J'(J'+1) - J''(J''+1)]$ is a running number of values $J''+1$ for a line in branch R or $-J''$ for a line in branch P. A sequence of signs of the rovibrational matrix moments $(+-+-++)$ is adopted in a similar way to that in a previous study.[20] Table 1 lists the rovibrational matrix elements derived from the experimental intensities and their experimental uncertainties. Finally, a fit of all listed rovibrational matrix elements to the system of linear Eq. (2) is carried out by using a least-squares fit program.[51] Six coefficients of the EDMF, $M_0, M_1, M_2, \ldots, M_5$, are determined, and the polynomial equation of the weighted EDMF is written as

$$\begin{aligned} M(x) \;=\; & 0.12261 - 3.59392x + 0.25488x^2 \\ & + 3.644204x^3 - 2.00256x^4 + 3.15384x^5, \end{aligned} \tag{4}$$

whereas the unweighted EDMF equation is

$$\begin{aligned} M(x) \;=\; & 0.12263 - 3.59385x + 0.24841x^2 \\ & + 3.66271x^3 - 1.6491x^4 - 1.96492x^5. \end{aligned} \tag{5}$$

Both equations implement an equilibrium separation of r_e = 1.12822 Å obtained from the constructed RKR potential. For comparison, the determined fitted EDMFs and those reported by Chung *et al*. are plotted against internuclear distance in Fig. 1.[20] Meanwhile, the theoretical EDMFs calculated through using the ACPF method at the aV6Z set level with the field values of ±0.005 a.u., those by Langhoff and Bauschlicher[36] through using the aug-cc-pVQZ ACPF-field method, and those by Ogilvie *et al*.[19] through using the MC-SCF method are all plotted in Fig. 1.

Table 1. Rovibrational transitional moments $M_{\upsilon 0}(m)$ of CO in units of Debye. The subscripts υ and 0 of $M_{\upsilon 0}(m)$ represent the υ-th upper vibrational level and the low vibrational level, respectively.

m	$M_{10}(m)$	$M_{20}(m)$	$M_{30}(m)$	$M_{40}(m)$	$M_{50}(m)$
–25			-3.64435×10^{-4}(1.15%)		
–24			-3.73484×10^{-4}(1.15%)		
–23	-1.08726×10^{-1}(3.56%)	6.1779×10^{-3}(0.75%)	-3.61098×10^{-4}(1.15%)		
–22	-1.06238×10^{-1}(3.56%)	6.2104×10^{-3}(0.75%)	-3.62795×10^{-4}(1.15%)		
–21	-1.07015×10^{-1}(3.56%)	6.2086×10^{-3}(0.75%)	-3.71995×10^{-4}(1.15%)		
–20	-1.06983×10^{-1}(3.56%)	6.2348×10^{-3}(0.75%)	-3.70620×10^{-4}(1.15%)		
–19	-1.07383×10^{-1}(3.56%)	6.2648×10^{-3}(0.75%)	-3.72714×10^{-4}(1.15%)		
–18	-1.06975×10^{-1}(3.56%)	6.2623×10^{-3}(0.75%)	-3.75246×10^{-4}(1.15%)		1.60845×10^{-6}(7.50%)
–17	-1.07315×10^{-1}(3.56%)	6.2799×10^{-3}(0.75%)	-3.77446×10^{-4}(1.15%)		2.04070×10^{-6}(7.50%)
–16	-1.06912×10^{-1}(3.56%)	6.2902×10^{-3}(0.75%)	-3.78924×10^{-4}(1.15%)	1.53506×10^{-5}(1.12%)	1.85821×10^{-6}(7.50%)
–15	-1.06990×10^{-1}(3.56%)	6.3071×10^{-3}(0.75%)	-3.82612×10^{-4}(1.15%)	1.66325×10^{-5}(1.12%)	1.63852×10^{-6}(7.50%)
–14	-1.07165×10^{-1}(3.56%)	6.3244×10^{-3}(0.75%)	-3.83036×10^{-4}(1.15%)	1.59628×10^{-5}(1.12%)	2.13755×10^{-6}(7.50%)
–13	-1.06891×10^{-1}(3.56%)	6.3361×10^{-3}(0.75%)	-3.85075×10^{-4}(1.15%)	1.63767×10^{-5}(1.12%)	1.86495×10^{-6}(7.50%)
–12	-1.07103×10^{-1}(3.56%)	6.3462×10^{-3}(0.75%)	-3.87080×10^{-4}(1.15%)		1.81283×10^{-6}(7.50%)
–11	-1.06915×10^{-1}(3.56%)	6.3645×10^{-3}(0.75%)	-3.90000×10^{-4}(1.15%)	1.63648×10^{-5}(1.12%)	1.80341×10^{-6}(7.50%)
–10	-1.06723×10^{-1}(3.56%)	6.3783×10^{-3}(0.75%)	-3.91620×10^{-4}(1.15%)	1.67650×10^{-5}(1.12%)	1.51588×10^{-6}(7.50%)
–9	-1.06834×10^{-1}(3.56%)	6.3910×10^{-3}(0.75%)	-3.93057×10^{-4}(1.15%)	1.72968×10^{-5}(1.12%)	1.23809×10^{-6}(7.50%)
–8	-1.06632×10^{-1}(3.56%)	6.4042×10^{-3}(0.75%)	-3.95541×10^{-4}(1.15%)	1.79460×10^{-5}(1.12%)	1.27906×10^{-6}(7.50%)
–7	-1.06658×10^{-1}(3.56%)	6.4192×10^{-3}(0.75%)	-3.97769×10^{-4}(1.15%)	1.79707×10^{-5}(1.12%)	1.19469×10^{-6}(7.50%)
–6	-1.06682×10^{-1}(3.56%)	6.4346×10^{-3}(0.75%)	-4.00914×10^{-4}(1.15%)	1.84099×10^{-5}(1.12%)	1.39754×10^{-6}(7.50%)
–5	-1.06681×10^{-1}(3.56%)	6.4500×10^{-3}(0.75%)	-4.03033×10^{-4}(1.15%)		1.13239×10^{-6}(7.50%)
–4	-1.06741×10^{-1}(3.56%)	6.4693×10^{-3}(0.75%)	-4.05679×10^{-4}(1.15%)	1.88807×10^{-5}(1.12%)	1.02759×10^{-6}(7.50%)
–3	-1.07319×10^{-1}(3.56%)	6.4836×10^{-3}(0.75%)	-4.09633×10^{-4}(1.15%)	1.89071×10^{-5}(1.12%)	1.13882×10^{-6}(7.50%)
–2	-1.06973×10^{-1}(3.56%)	6.5057×10^{-3}(0.75%)	-4.09918×10^{-4}(1.15%)	1.93609×10^{-5}(1.12%)	
–1	-1.06050×10^{-1}(3.56%)	6.5284×10^{-3}(0.75%)	-4.12978×10^{-4}(1.15%)	2.04822×10^{-5}(1.12%)	
1	-1.06567×10^{-1}(3.56%)	6.5570×10^{-3}(0.75%)	-4.17436×10^{-4}(1.15%)	2.05012×10^{-5}(1.12%)	
2	-1.06796×10^{-1}(3.56%)	6.5739×10^{-3}(0.75%)	-4.20988×10^{-4}(1.15%)	2.10375×10^{-5}(1.12%)	
3	-1.06837×10^{-1}(3.56%)	6.5871×10^{-3}(0.75%)	-4.23839×10^{-4}(1.15%)	2.18628×10^{-5}(1.12%)	
4	-1.06885×10^{-1}(3.56%)	6.6033×10^{-3}(0.75%)	-4.25765×10^{-4}(1.15%)	2.18107×10^{-5}(1.12%)	
5	-1.06971×10^{-1}(3.56%)	6.6186×10^{-3}(0.75%)	-4.27207×10^{-4}(1.15%)	2.22226×10^{-5}(1.12%)	
6	-1.06896×10^{-1}(3.56%)	6.6342×10^{-3}(0.75%)	-4.29007×10^{-4}(1.15%)	2.26652×10^{-5}(1.12%)	
7	-1.07024×10^{-1}(3.56%)	6.6523×10^{-3}(0.75%)	-4.31103×10^{-4}(1.15%)	2.27348×10^{-5}(1.12%)	
8	-1.07013×10^{-1}(3.56%)	6.6690×10^{-3}(0.75%)	-4.32796×10^{-4}(1.15%)		
9	-1.06924×10^{-1}(3.56%)	6.6868×10^{-3}(0.75%)	-4.34849×10^{-4}(1.15%)	2.33833×10^{-5}(1.12%)	
10	-1.07149×10^{-1}(3.56%)	6.7081×10^{-3}(0.75%)	-4.39387×10^{-4}(1.15%)	2.33329×10^{-5}(1.12%)	
11	-1.07190×10^{-1}(3.56%)	6.7256×10^{-3}(0.75%)	-4.42360×10^{-4}(1.15%)	2.41239×10^{-5}(1.12%)	
12	-1.07395×10^{-1}(3.56%)	6.7442×10^{-3}(0.75%)	-4.44085×10^{-4}(1.15%)	2.50118×10^{-5}(1.12%)	
13	-1.07425×10^{-1}(3.56%)	6.7650×10^{-3}(0.75%)	-4.49534×10^{-4}(1.15%)	2.48110×10^{-5}(1.12%)	
14	-1.07512×10^{-1}(3.56%)	6.7867×10^{-3}(0.75%)	-4.51383×10^{-4}(1.15%)	2.52936×10^{-5}(1.12%)	
15	-1.07630×10^{-1}(3.56%)	6.8046×10^{-3}(0.75%)	-4.55507×10^{-4}(1.15%)		
16	-1.07721×10^{-1}(3.56%)	6.8255×10^{-3}(0.75%)	-4.58738×10^{-4}(1.15%)	2.59868×10^{-5}(1.12%)	
17	-1.07670×10^{-1}(3.56%)	6.8486×10^{-3}(0.75%)	-4.60818×10^{-4}(1.15%)		
18	-1.07456×10^{-1}(3.56%)	6.8658×10^{-3}(0.75%)	-4.64357×10^{-4}(1.15%)		
19	-1.08000×10^{-1}(3.56%)	6.8886×10^{-3}(0.75%)	-4.67094×10^{-4}(1.15%)		
20	-1.08020×10^{-1}(3.56%)	6.9086×10^{-3}(0.75%)	-4.71070×10^{-4}(1.15%)		
21	-1.08247×10^{-1}(3.56%)	6.9296×10^{-3}(0.75%)	-4.72801×10^{-4}(1.15%)		
22	-1.08250×10^{-1}(3.56%)	6.9462×10^{-3}(0.75%)	-4.77859×10^{-4}(1.15%)		
23	-1.08915×10^{-1}(3.56%)	6.9589×10^{-3}(0.75%)	-4.77188×10^{-4}(1.15%)		
24	-1.09055×10^{-1}(3.56%)		-4.78968×10^{-4}(1.15%)		

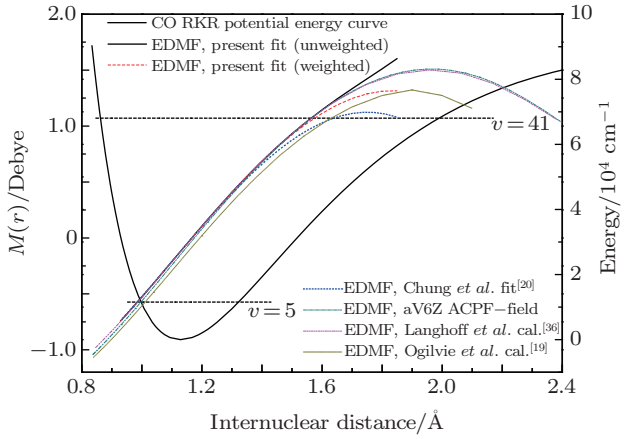


Fig. 1. (color online) Electric dipole moment functions and RKR potential energy curve.

Within the respective valid range, the three fitted EDMFs are in close agreement with each other. According to the RKR potential, the classical turning points of the vibrational level $\upsilon = 5$ are found to be approximately 0.967 Å and 1.322 Å. Therefore, the fitted EDMF is most reliable in the region between these two limits, which are slightly different from the results shown in Chung *et al*. (0.99 Å and 1.33 Å).[20] The valid range of the fitted EDMF is controlled by the largest overtones which are very sensitive to determining the higher coefficients of M_i in Eq. (1). Thus, it is important to obtain experimental measurements for the largest possible values of υ' and $\Delta\upsilon$. The weighted and unweighted fitted EDMFs overlap together at 0.85 Å$\leq r \leq$ 1.45 Å in the present work. In the valid range, all the fitted EDMFs agree well with the theoretical EDMF calculated using the ACPF method with a finite-field $\pm$0.005 a.u at the aV6Z basis set level (aV6Z ACPF-field). They also agree well with the theoretical results of Langhoff and Bauschlicher.[36] The three lines outside the valid range are not consistent with the two theoretical EDMFs at large internuclear distances. Actually, the degree of agreement between the fitted EDMF of Chung *et al*. and the two theoretical EDMFs become continually worse when $r \geq 1.33$ Å.

3.2. Theoretical results of EDMFs

According to geometrical optimization of the CO molecule, the equilibrium separation and the minimum energy are 1.1324 Å and −113.197964 a.u. for the aV6Z basis set, and 1.1323 Å and −113.198196 a.u for the spdfghi aV6Z basis set, respectively. These two values of r_e agree well with the experimental values of 1.1283 Å and 1.1282 Å obtained from the constructed RKR potential in the present work.[52] The calculated energies and dipole moments each as a function of r are listed in Table 2 at the ACPF (4220) level using the aV6Z and spdfghi aV6Z basis sets. The two EDMFs almost converge both with and without using the finite-field approach. Here, we only compare the aV6Z ACPF-field EDMF with the three fitted and previous theoretical ones in Fig. 1.

Table 2. Energies and electric dipole moments (EDMs) (a.u.)[a] for the $X^1\Sigma^+$ state CO using the aug–cc–pV6Z and spdfgh aug–cc–pV6Z basis sets.

$r(a_0)$	aV6Z			spdfghi aV6Z		
	Energy/a.u.	EDM	EDM (field)	Energy/a.u.	EDM	EDM (field)
1.5022	–112.594710	–0.434729	–0.538579	–112.597530	–0.432539	–0.538746
1.5396	–112.694260	–0.416295	–0.526169	–112.697154	–0.413896	–0.526399
1.5771	–112.779349	–0.404725	–0.426192	–112.784017	–0.395134	–0.440991
1.6129	–112.849758	–0.385034	–0.392749	–112.852724	–0.381194	–0.392764
1.6564	–112.922746	–0.360298	–0.367594	–112.925744	–0.356304	–0.367608
1.6932	–112.974897	–0.338773	–0.345766	–112.977921	–0.334650	–0.345780
1.7299	–113.019118	–0.316863	–0.323584	–113.022169	–0.312614	–0.323597
1.7606	–113.051005	–0.298063	–0.304616	–113.054078	–0.293758	–0.304628
1.7990	–113.084844	–0.274235	–0.280528	–113.087944	–0.269806	–0.280539
1.8224	–113.102516	–0.259524	–0.265659	–113.105632	–0.255022	–0.265670
1.8498	–113.120705	–0.242073	–0.248020	–113.123841	–0.237484	–0.248030
1.8832	–113.139432	–0.220618	–0.226331	–113.142591	–0.215926	–0.226341
1.9264	–113.158734	–0.192552	–0.197949	–113.161924	–0.187730	–0.197959
1.9907	–113.178715	–0.150241	–0.155138	–113.181949	–0.145231	–0.155146
2.0203	–113.184896	–0.130654	–0.135304	–113.188149	–0.125561	–0.135313
2.0472	–113.189104	–0.112747	–0.117171	–113.192376	–0.107502	–0.117180
2.0930	–113.193494	–0.082217	–0.086238	–113.196797	–0.076842	–0.086246
2.1735	–113.194179	–0.028640	–0.031914	–113.197536	–0.023047	–0.031921
2.2276	–113.190630	0.007105	0.004354	–113.194024	0.012835	0.004348
2.2628	–113.186938	0.030311	0.027802	–113.190356	0.036040	0.027796
2.3048	–113.181341	0.057660	0.055558	–113.184788	0.063478	0.055553
2.4112	–113.162691	0.125508	0.124413	–113.166209	0.131494	0.124408
2.4974	–113.144321	0.178495	0.178223	–113.147899	0.184669	0.178219

Table 2. (*Continued*).

$r(a_0)$	aV6Z			spdfghi aV6Z		
	Energy/a.u.	EDM	EDM (field)	Energy/a.u.	EDM	EDM (field)
2.5748	–113.126332	0.224230	0.224670	–113.129961	0.230504	0.224667
2.6473	–113.108754	0.265272	0.266354	–113.112432	0.271622	0.266352
2.7169	–113.091603	0.302829	0.304503	–113.095327	0.309239	0.304502
2.7846	–113.074884	0.337664	0.339788	–113.078653	0.344024	0.339789
2.8511	–113.058602	0.370032	0.372609	–113.062416	0.376429	0.372611
2.9170	–113.042757	0.400190	0.403210	–113.046615	0.406612	0.403215
2.9826	–113.027352	0.428309	0.431728	–113.031253	0.434840	0.431735
3.0483	–113.012384	0.454454	0.458231	–113.016329	0.460998	0.458241
3.1143	–112.997852	0.478616	0.482739	–113.001840	0.485196	0.482751
3.1810	–112.983754	0.500774	0.505215	–112.987785	0.507406	0.505228
3.2484	–112.970089	0.520847	0.525579	–112.974163	0.527593	0.525594
3.3167	–112.956859	0.539021	0.543707	–112.960975	0.545584	0.543724
3.3863	–112.944062	0.554580	0.559440	–112.948221	0.561197	0.559459
3.4572	–112.931700	0.567516	0.572564	–112.935901	0.574287	0.572584
3.5298	–112.919774	0.577580	0.582850	–112.924016	0.584470	0.582870
3.6042	–112.908286	0.584327	0.589987	–112.912569	0.591417	0.590005
3.6806	–112.897239	0.587511	0.593662	–112.901561	0.594701	0.593680
3.7595	–112.886635	0.586470	0.593498	–112.890995	0.594123	0.593515
3.8411	–112.876480	0.580907	0.589076	–112.880875	0.588810	0.589090
3.9259	–112.866780	0.570119	0.579950	–112.871206	0.578305	0.579960
4.0143	–112.857540	0.553588	0.565654	–112.861993	0.562088	0.565660
4.1070	–112.848771	0.530930	0.545731	–112.853245	0.539840	0.545731
4.2047	–112.840482	0.501952	0.519776	–112.844971	0.510937	0.519768
4.3084	–112.832687	0.466245	0.487520	–112.837182	0.475143	0.487503
4.4195	–112.825401	0.424333	0.448937	–112.829894	0.433342	0.448909
4.5396	–112.818642	0.377221	0.404351	–112.823123	0.385900	0.404314
4.6711	–112.812428	0.325645	0.354639	–112.816888	0.333875	0.354594
4.8172	–112.806776	0.271049	0.301427	–112.811208	0.278671	0.301378
4.9828	–112.801702	0.215163	0.196298	–112.806097	0.221749	0.196166

[a] A minus sign implies C^-O^+ polarity.

The aV6Z ACPF-field EDMF agrees well with the three fitted ones in their valid ranges. Compared with the theoretical results given by Langhoff and Bauschlicher,[36] the values of the dipole moments are smaller at small r and slightly larger at large r. The latest work of Oglivie *et al.*[19] disagrees with the three fitted and the two theoretical ones.

3.3. Calculations of transition matrix moments

First, by combining the RKR potential and the EDMFs of Chung *et al.*,[20] and Langhoff and Bauschlicher,[36] and the present fits, we calculate the rovibrational matrix moments and vibrational matrix moments. In Table 3, the absolute values of some vibrational matrix elements $\mu_{\upsilon',\upsilon''}$ are compared with the experimental results. The values $|\mu_{\upsilon',\upsilon''}|$ calculated using the present unweighted fitted EDMF agree well with the experimental values at the bands υ'–0 ($\upsilon' = 0$–5). Though the values derived using the weighted fitted EDMF also agree well with the measurements at the bands υ'–0 ($\upsilon' = 0$–4), the value $|\mu_{5-0}| = 2.471 \times 10^{-6}$ Debye deviates largely from the experimental value of 1.079×10^{-6} Debye. One possible reason is that Chung *et al.* did not specify the experimental uncertainty and only provided a minimum uncertainty of about 15% for all measured line intensities in their work.[20] Thus, only the unweighted fitted EDMF will be considered when comparing line intensities later in the article.

Further, we calculate vibrational dipole moments by combining the *ab initio* potential and the *ab initio* electric dipole moments for the ground state CO in Table 4. Without a finite-field, both the results of the aV6Z and spdfghi aV6Z EDMFs only agree well with the experimental values in the bands υ'–0 ($\upsilon' = 0$–3). When adding the finite-field, the values $\mu_{\upsilon',\upsilon''}$ agree well with measurements not only in the bands υ'–0 ($\upsilon' = 0$–3) but also in the 4–0 and 5–0 bands. The vibrational dipole moments, calculated using the aV6Z ACPF-field EDMF, seems better than using the spdfghi aV6Z ACPF-field EDMF. Thus, the aV6Z ACPF-field EDMF is used to compute the rovibrational transition moments and line intensities by combining the RKR potential. In Table 3, by comparing the $\mu_{\upsilon',\upsilon''}$ calculated using the aV6Z ACPF-field EDMF and the EDMF of Langhoff *et al.* with experimental results, it is clear that our $\mu_{\upsilon',\upsilon''}$ is in better agreement with the experimental results except the value of $\mu_{0,0}$. Relative to the approach without the finite-field, the variation of the electric dipole moment calculated using a finite-field approach is larger at the equilibrium separation than at other separations. This may be the reason why the value $\mu_{0,0}$ is so much different from the fitted ones.

Table 3. Vibrational dipole moments $|\mu_{v',v''}|$ (in Debye) computed by combining the RKR potential and the EDMFs for vibrational bands of CO.

$v'-v''$	Predictions of $\|\mu_{v',v''}\|$ from EDMF					Experiments			
	This fit[a]	This fit[b]	Chung *et al.*[c]	This acpf[d]	Langhoff *et al.*[e]	Ref. [38]	Ref. [22]	Others	Ref.
0–0	1.098×10^{-1}	1.098×10^{-1}	1.098×10^{-1}	1.260×10^{-1}	1.120×10^{-1}		1.098×10^{-1}		
1–0	1.071×10^{-1}	1.071×10^{-1}	1.060×10^{-1}	1.091×10^{-1}	1.077×10^{-1}	1.060×10^{-1}	1.084×10^{-1}		
2–0	6.536×10^{-3}	6.544×10^{-3}	6.668×10^{-3}	6.585×10^{-3}	6.538×10^{-3}	6.646×10^{-3}	6.600×10^{-3}	6.631×10^{-3}	[9]
								6.533×10^{-3}	[41]
3–0	4.167×10^{-4}	4.133×10^{-4}	4.085×10^{-4}	4.154×10^{-4}	3.974×10^{-4}	4.097×10^{-4}	4.290×10^{-4}	4.101×10^{-4}	[13]
								4.090×10^{-4}	[14]
								4.090×10^{-4}	[16]
								4.139×10^{-4}	[15]
								4.139×10^{-4}	[53]
								4.136×10^{-4}	
								4.138×10^{-4}	[17]
4–0	2.022×10^{-5}	2.003×10^{-5}	2.073×10^{-5}	2.051×10^{-5}	2.160×10^{-5}	2.088×10^{-5}	2.016×10^{-5}	2.012×10^{-5}	[18]
5–0	1.100×10^{-6}	2.471×10^{-6}	1.099×10^{-6}	1.106×10^{-6}	2.149×10^{-5}			1.079×10^{-6}	[20]

[a]The results are derived from the unweighted fitted EDMF in this work.

[b]The results are derived from the weighted fitted EDMF in this work.

[c]The values are obtained using the EDMF of Chung *et al.*[20]

[d]The values are obtained using the present aV6Z ACPF–field EDMF.

[e]The values are obtained using the EDMF of Langhoff *et al.*[36]

Table 4. Vibrational dipole moments $\mu_{v',v''}$ (Debye) computed by combining the *ab initio* potential and the *ab initio* electric dipole moments for the ground state CO.

$v'-v''$	aV6Z	aV6Z (field)	spdfgh aV6Z	spdfgh aV6Z (field)	$v'-v''$	aV6Z	aV6Z (field)	spdfgh aV6Z	spdfgh aV6Z (field)
0–0	1.0300×10^{-1}	1.2590×10^{-1}	1.0302×10^{-1}	1.2596×10^{-1}					
1–1	7.7193×10^{-2}	9.9759×10^{-2}	7.7213×10^{-2}	9.9816×10^{-2}	1–0	-1.0832×10^{-1}	-1.0939×10^{-1}	-1.0832×10^{-1}	-1.0939×10^{-1}
2–2	5.1363×10^{-2}	7.3546×10^{-2}	5.1381×10^{-2}	7.3600×10^{-2}	2–1	-1.5307×10^{-1}	-1.5458×10^{-1}	-1.5307×10^{-1}	-1.5458×10^{-1}
3–3	2.5438×10^{-2}	4.7266×10^{-2}	2.5457×10^{-2}	4.7318×10^{-2}	3–2	-1.8727×10^{-1}	-1.8913×10^{-1}	-1.8727×10^{-1}	-1.8914×10^{-1}
4–4	-5.8012×10^{-4}	2.0928×10^{-2}	-5.6199×10^{-4}	2.0978×10^{-2}	4–3	-2.1593×10^{-1}	-2.1812×10^{-1}	-2.1593×10^{-1}	-2.1813×10^{-1}
5–5	-2.6627×10^{-2}	-5.4637×10^{-3}	-2.6609×10^{-2}	-5.4155×10^{-3}	5–4	-2.4105×10^{-1}	-2.4351×10^{-1}	-2.4104×10^{-1}	-2.4351×10^{-1}
6–6	-5.2716×10^{-2}	-3.1896×10^{-2}	-5.2697×10^{-2}	-3.1849×10^{-2}	6–5	-2.6359×10^{-1}	-2.6629×10^{-1}	-2.6359×10^{-1}	-2.6630×10^{-1}
7–7	-7.8836×10^{-2}	-5.8361×10^{-2}	-7.8817×10^{-2}	-5.8315×10^{-2}	7–6	-2.8413×10^{-1}	-2.8707×10^{-1}	-2.8412×10^{-1}	-2.8707×10^{-1}
8–8	-1.0498×10^{-1}	-8.4853×10^{-2}	-1.0496×10^{-1}	-8.4809×10^{-2}	8–7	-3.0304×10^{-1}	-3.0621×10^{-1}	-3.0303×10^{-1}	-3.0621×10^{-1}
9–9	-1.3114×10^{-1}	-1.1137×10^{-1}	-1.3112×10^{-1}	-1.1132×10^{-1}	9–8	-3.2059×10^{-1}	-3.2398×10^{-1}	-3.2058×10^{-1}	-3.2399×10^{-1}
10–10	-1.5731×10^{-1}	-1.3789×10^{-1}	-1.5729×10^{-1}	-1.3785×10^{-1}	10–9	-3.3697×10^{-1}	-3.4057×10^{-1}	-3.3696×10^{-1}	-3.4057×10^{-1}
11–11	-1.8349×10^{-1}	-1.6442×10^{-1}	-1.8347×10^{-1}	-1.6438×10^{-1}	11–10	-3.5232×10^{-1}	-3.5611×10^{-1}	-3.5231×10^{-1}	-3.5612×10^{-1}
12–12	-2.0965×10^{-1}	-1.9094×10^{-1}	-2.0963×10^{-1}	-1.9090×10^{-1}	12–11	-3.6674×10^{-1}	-3.7072×10^{-1}	-3.6672×10^{-1}	-3.7073×10^{-1}
13–13	-2.3579×10^{-1}	-2.1743×10^{-1}	-2.3577×10^{-1}	-2.1740×10^{-1}	13–12	-3.8031×10^{-1}	-3.8448×10^{-1}	-3.8029×10^{-1}	-3.8449×10^{-1}
14–14	-2.6191×10^{-1}	-2.4390×10^{-1}	-2.6189×10^{-1}	-2.4387×10^{-1}	14–13	-3.9310×10^{-1}	-3.9744×10^{-1}	-3.9308×10^{-1}	-3.9745×10^{-1}
15–15	-2.8799×10^{-1}	-2.7033×10^{-1}	-2.8797×10^{-1}	-2.7030×10^{-1}	15–14	-4.0516×10^{-1}	-4.0966×10^{-1}	-4.0514×10^{-1}	-4.0967×10^{-1}
16–16	-3.1403×10^{-1}	-2.9671×10^{-1}	-3.1401×10^{-1}	-2.9668×10^{-1}	16–15	-4.1653×10^{-1}	-4.2119×10^{-1}	-4.1652×10^{-1}	-4.2120×10^{-1}
17–17	-3.4000×10^{-1}	-3.2302×10^{-1}	-3.3998×10^{-1}	-3.2300×10^{-1}	17–16	-4.2725×10^{-1}	-4.3204×10^{-1}	-4.2723×10^{-1}	-4.3206×10^{-1}
18–18	-3.6591×10^{-1}	-3.4926×10^{-1}	-3.6589×10^{-1}	-3.4924×10^{-1}	18–17	-4.3733×10^{-1}	-4.4226×10^{-1}	-4.3731×10^{-1}	-4.4227×10^{-1}
19–19	-3.9173×10^{-1}	-3.7541×10^{-1}	-3.9172×10^{-1}	-3.7539×10^{-1}	19–18	-4.4680×10^{-1}	-4.5185×10^{-1}	-4.4679×10^{-1}	-4.5187×10^{-1}
20–20	-4.1746×10^{-1}	-4.0145×10^{-1}	-4.1745×10^{-1}	-4.0144×10^{-1}	20–19	-4.5569×10^{-1}	-4.6084×10^{-1}	-4.5567×10^{-1}	-4.6085×10^{-1}
21–21	-4.4307×10^{-1}	-4.2738×10^{-1}	-4.4305×10^{-1}	-4.2737×10^{-1}	21–20	-4.6398×10^{-1}	-4.6923×10^{-1}	-4.6396×10^{-1}	-4.6925×10^{-1}
22–22	-4.6853×10^{-1}	-4.5317×10^{-1}	-4.6852×10^{-1}	-4.5316×10^{-1}	22–21	-4.7168×10^{-1}	-4.7703×10^{-1}	-4.7166×10^{-1}	-4.7705×10^{-1}
23–23	-4.9384×10^{-1}	-4.7880×10^{-1}	-4.9383×10^{-1}	-4.7880×10^{-1}	23–22	-4.7880×10^{-1}	-4.8425×10^{-1}	-4.7878×10^{-1}	-4.8427×10^{-1}
24–24	-5.1899×10^{-1}	-5.0426×10^{-1}	-5.1898×10^{-1}	-5.0426×10^{-1}	24–23	-4.8535×10^{-1}	-4.9089×10^{-1}	-4.8533×10^{-1}	-4.9091×10^{-1}
25–25	-5.4396×10^{-1}	-5.2954×10^{-1}	-5.4394×10^{-1}	-5.2954×10^{-1}	25–24	-4.9133×10^{-1}	-4.9694×10^{-1}	-4.9131×10^{-1}	-4.9696×10^{-1}
26–26	-5.6872×10^{-1}	-5.5460×10^{-1}	-5.6870×10^{-1}	-5.5459×10^{-1}	26–25	-4.9673×10^{-1}	-5.0241×10^{-1}	-4.9671×10^{-1}	-5.0243×10^{-1}
27–27	-5.9326×10^{-1}	-5.7942×10^{-1}	-5.9323×10^{-1}	-5.7941×10^{-1}	27–26	-5.0154×10^{-1}	-5.0727×10^{-1}	-5.0153×10^{-1}	-5.0730×10^{-1}

Table 4. (*Continued*).

υ'–υ''	aV6Z	aV6Z (field)	spdfgh aV6Z	spdfgh aV6Z (field)	υ'–υ''	aV6Z	aV6Z (field)	spdfgh aV6Z	spdfgh aV6Z (field)
2–0	6.5975×10^{-3}	6.6076×10^{-3}	6.5980×10^{-3}	6.6081×10^{-3}					
3–1	1.1604×10^{-2}	1.1587×10^{-2}	1.1605×10^{-2}	1.1588×10^{-2}	3–0	-4.3002×10^{-4}	-4.1623×10^{-4}	-4.3025×10^{-4}	-4.1648×10^{-4}
4–2	1.6600×10^{-2}	1.6592×10^{-2}	1.6601×10^{-2}	1.6593×10^{-2}	4–1	-8.9315×10^{-4}	-8.5829×10^{-4}	-8.9344×10^{-4}	-8.5860×10^{-4}
5–3	2.1643×10^{-2}	2.1683×10^{-2}	2.1644×10^{-2}	2.1684×10^{-2}	5–2	-1.4294×10^{-3}	-1.4008×10^{-3}	-1.4301×10^{-3}	-1.4013×10^{-3}
6–4	2.6809×10^{-2}	2.6872×10^{-2}	2.6810×10^{-2}	2.6873×10^{-2}	6–3	-2.0851×10^{-3}	-2.0406×10^{-3}	-2.0859×10^{-3}	-2.0413×10^{-3}
7–5	3.2076×10^{-2}	3.2165×10^{-2}	3.2077×10^{-2}	3.2166×10^{-2}	7–4	-2.8417×10^{-3}	-2.7788×10^{-3}	-2.8425×10^{-3}	-2.7797×10^{-3}
8–6	3.7444×10^{-2}	3.7562×10^{-2}	3.7445×10^{-2}	3.7563×10^{-2}	8–5	-3.6819×10^{-3}	-3.6169×10^{-3}	-3.6827×10^{-3}	-3.6179×10^{-3}
9–7	4.2912×10^{-2}	4.3062×10^{-2}	4.2913×10^{-2}	4.3063×10^{-2}	9–6	-4.6174×10^{-3}	-4.5557×10^{-3}	-4.6184×10^{-3}	-4.5568×10^{-3}
10–8	4.8479×10^{-2}	4.8662×10^{-2}	4.8480×10^{-2}	4.8663×10^{-2}	10–7	-5.6589×10^{-3}	-5.5969×10^{-3}	-5.6600×10^{-3}	-5.5980×10^{-3}
11–9	5.4140×10^{-2}	5.4361×10^{-2}	5.4141×10^{-2}	5.4362×10^{-2}	11–8	-6.8089×10^{-3}	-6.7417×10^{-3}	-6.8102×10^{-3}	-6.7429×10^{-3}
12–10	5.9891×10^{-2}	6.0155×10^{-2}	5.9892×10^{-2}	6.0156×10^{-2}	12–9	-8.0621×10^{-3}	-7.9920×10^{-3}	-8.0634×10^{-3}	-7.9932×10^{-3}
13–11	6.5732×10^{-2}	6.6041×10^{-2}	6.5733×10^{-2}	6.6042×10^{-2}	13–10	-9.4197×10^{-3}	-9.3488×10^{-3}	-9.4211×10^{-3}	-9.3501×10^{-3}
14–12	7.1656×10^{-2}	7.2014×10^{-2}	7.1657×10^{-2}	7.2016×10^{-2}	14–11	-1.0886×10^{-2}	-1.0814×10^{-2}	-1.0887×10^{-2}	-1.0815×10^{-2}
15–13	7.7657×10^{-2}	7.8074×10^{-2}	7.7658×10^{-2}	7.8076×10^{-2}	15–12	-1.2463×10^{-2}	-1.2388×10^{-2}	-1.2465×10^{-2}	-1.2389×10^{-2}
16–14	8.3731×10^{-2}	8.4216×10^{-2}	8.3732×10^{-2}	8.4218×10^{-2}	16–13	-1.4155×10^{-2}	-1.4073×10^{-2}	-1.4156×10^{-2}	-1.4075×10^{-2}
17–15	8.9881×10^{-2}	9.0436×10^{-2}	8.9882×10^{-2}	9.0438×10^{-2}	17–14	-1.5958×10^{-2}	-1.5871×10^{-2}	-1.5960×10^{-2}	-1.5873×10^{-2}
18–16	9.6104×10^{-2}	9.6730×10^{-2}	9.6106×10^{-2}	9.6732×10^{-2}	18–15	-1.7869×10^{-2}	-1.7783×10^{-2}	-1.7871×10^{-2}	-1.7785×10^{-2}
19–17	1.0239×10^{-1}	1.0310×10^{-1}	1.0239×10^{-1}	1.0310×10^{-1}	19–16	-1.9892×10^{-2}	-1.9809×10^{-2}	-1.9894×10^{-2}	-1.9811×10^{-2}
20–18	1.0874×10^{-1}	1.0953×10^{-1}	1.0874×10^{-1}	1.0953×10^{-1}	20–17	-2.2034×10^{-2}	-2.1951×10^{-2}	-2.2037×10^{-2}	-2.1954×10^{-2}
21–19	1.1514×10^{-1}	1.1603×10^{-1}	1.1514×10^{-1}	1.1603×10^{-1}	21–18	-2.4294×10^{-2}	-2.4209×10^{-2}	-2.4297×10^{-2}	-2.4212×10^{-2}
22–20	1.2162×10^{-1}	1.2259×10^{-1}	1.2162×10^{-1}	1.2259×10^{-1}	22–19	-2.6658×10^{-2}	-2.6584×10^{-2}	-2.6662×10^{-2}	-2.6587×10^{-2}
23–21	1.2816×10^{-1}	1.2921×10^{-1}	1.2816×10^{-1}	1.2921×10^{-1}	23–20	-2.9127×10^{-2}	-2.9077×10^{-2}	-2.9131×10^{-2}	-2.9080×10^{-2}
24–22	1.3474×10^{-1}	1.3588×10^{-1}	1.3475×10^{-1}	1.3588×10^{-1}	24–21	-3.1710×10^{-2}	-3.1687×10^{-2}	-3.1714×10^{-2}	-3.1690×10^{-2}
25–23	1.4138×10^{-1}	1.4260×10^{-1}	1.4138×10^{-1}	1.4260×10^{-1}	25–22	-3.4415×10^{-2}	-3.4417×10^{-2}	-3.4420×10^{-2}	-3.4420×10^{-2}
26–24	1.4805×10^{-1}	1.4937×10^{-1}	1.4805×10^{-1}	1.4937×10^{-1}	26–23	-3.7238×10^{-2}	-3.7265×10^{-2}	-3.7243×10^{-2}	-3.7268×10^{-2}
27–25	1.5477×10^{-1}	1.5618×10^{-1}	1.5477×10^{-1}	1.5619×10^{-1}	27–24	-4.0179×10^{-2}	-4.0232×10^{-2}	-4.0183×10^{-2}	-4.0234×10^{-2}
4–0	4.3121×10^{-5}	2.0117×10^{-5}	4.3239×10^{-5}	2.0109×10^{-5}					
5–1	6.4749×10^{-5}	5.0673×10^{-5}	6.4853×10^{-5}	5.0835×10^{-5}	5–0	-1.3562×10^{-5}	1.5796×10^{-6}	-1.3569×10^{-5}	1.6439×10^{-6}
6–2	8.2069×10^{-5}	9.6781×10^{-5}	8.2208×10^{-5}	9.7039×10^{-5}	6–1	4.2863×10^{-6}	1.1173×10^{-6}	4.1952×10^{-6}	1.1258×10^{-6}
7–3	1.5700×10^{-4}	1.5733×10^{-4}	1.5716×10^{-4}	1.5755×10^{-4}	7–2	9.3291×10^{-6}	1.2481×10^{-6}	9.3150×10^{-6}	1.1530×10^{-6}
8–4	2.5286×10^{-4}	2.3848×10^{-4}	2.5303×10^{-4}	2.3871×10^{-4}	8–3	5.7541×10^{-6}	1.0362×10^{-6}	5.8363×10^{-6}	8.7791×10^{-7}
9–5	3.6570×10^{-4}	3.4242×10^{-4}	3.6595×10^{-4}	3.4275×10^{-4}	9–4	8.4889×10^{-6}	-1.7618×10^{-6}	8.5743×10^{-6}	-1.8874×10^{-6}
10–6	4.9963×10^{-4}	4.7076×10^{-4}	4.9997×10^{-4}	4.7117×10^{-4}	10–5	5.6864×10^{-6}	-7.5951×10^{-6}	5.6996×10^{-6}	-7.6883×10^{-6}
11–7	6.6072×10^{-4}	6.2627×10^{-4}	6.6110×10^{-4}	6.2670×10^{-4}	11–6	-7.5834×10^{-6}	-1.6902×10^{-5}	-7.6435×10^{-6}	-1.6985×10^{-5}
12–8	8.5183×10^{-4}	8.1260×10^{-4}	8.5220×10^{-4}	8.1302×10^{-4}	12–7	-2.9432×10^{-5}	-3.0188×10^{-5}	-2.9530×10^{-5}	-3.0258×10^{-5}
13–9	1.0758×10^{-3}	1.0329×10^{-3}	1.0762×10^{-3}	1.0334×10^{-3}	13–8	-5.3416×10^{-5}	-4.8833×10^{-5}	-5.3504×10^{-5}	-4.8891×10^{-5}
14–10	1.3370×10^{-3}	1.2899×10^{-3}	1.3374×10^{-3}	1.2904×10^{-3}	14–9	-8.1836×10^{-5}	-7.4069×10^{-5}	-8.1896×10^{-5}	-7.4121×10^{-5}
15–11	1.6373×10^{-3}	1.5867×10^{-3}	1.6378×10^{-3}	1.5873×10^{-3}	15–10	-1.1912×10^{-4}	-1.0720×10^{-4}	-1.1915×10^{-4}	-1.0726×10^{-4}
16–12	1.9772×10^{-3}	1.9269×10^{-3}	1.9778×10^{-3}	1.9276×10^{-3}	16–11	-1.6789×10^{-4}	-1.4968×10^{-4}	-1.6790×10^{-4}	-1.4977×10^{-4}
17–13	2.3626×10^{-3}	2.3135×10^{-3}	2.3634×10^{-3}	2.3143×10^{-3}	17–12	-2.2786×10^{-4}	-2.0335×10^{-4}	-2.2790×10^{-4}	-2.0350×10^{-4}
18–14	2.8027×10^{-3}	2.7498×10^{-3}	2.8037×10^{-3}	2.7507×10^{-3}	18–13	-2.9749×10^{-4}	-2.7016×10^{-4}	-2.9761×10^{-4}	-2.7035×10^{-4}
19–15	3.3002×10^{-3}	3.2393×10^{-3}	3.3013×10^{-3}	3.2404×10^{-3}	19–14	-3.7761×10^{-4}	-3.5210×10^{-4}	-3.7784×10^{-4}	-3.5232×10^{-4}
20–16	3.8510×10^{-3}	3.7858×10^{-3}	3.8523×10^{-3}	3.7870×10^{-3}	20–15	-4.7599×10^{-4}	-4.5103×10^{-4}	-4.7635×10^{-4}	-4.5130×10^{-4}
21–17	4.4579×10^{-3}	4.3929×10^{-3}	4.4594×10^{-3}	4.3942×10^{-3}	21–16	-5.9908×10^{-4}	-5.6895×10^{-4}	-5.9959×10^{-4}	-5.6931×10^{-4}
22–18	5.1341×10^{-3}	5.0639×10^{-3}	5.1359×10^{-3}	5.0653×10^{-3}	22–17	-7.4290×10^{-4}	-7.0835×10^{-4}	-7.4358×10^{-4}	-7.0879×10^{-4}
23–19	5.8882×10^{-3}	5.8019×10^{-3}	5.8904×10^{-3}	5.8035×10^{-3}	23–18	-9.0212×10^{-4}	-8.7207×10^{-4}	-9.0296×10^{-4}	-8.7254×10^{-4}
24–20	6.7151×10^{-3}	6.6104×10^{-3}	6.7176×10^{-3}	6.6120×10^{-3}	24–19	-1.0852×10^{-3}	-1.0631×10^{-3}	-1.0862×10^{-3}	-1.0635×10^{-3}
25–21	7.6080×10^{-3}	7.4927×10^{-3}	7.6107×10^{-3}	7.4943×10^{-3}	25–20	-1.3069×10^{-3}	-1.2842×10^{-3}	-1.3082×10^{-3}	-1.2845×10^{-3}
26–22	8.5716×10^{-3}	8.4526×10^{-3}	8.5743×10^{-3}	8.4542×10^{-3}	26–21	-1.5711×10^{-3}	-1.5382×10^{-3}	-1.5725×10^{-3}	-1.5385×10^{-3}
27–23	9.6142×10^{-3}	9.4936×10^{-3}	9.6167×10^{-3}	9.4953×10^{-3}	27–22	-1.8730×10^{-3}	-1.8282×10^{-3}	-1.8744×10^{-3}	-1.8285×10^{-3}

Finally, the Herman–Wallis factors of CO calculated using the present unweighted fitted EDMF and aV6Z ACPF-field EDMF are compared with the measurements of Ogilvie *et al*. for the bands υ'–0 ($\upsilon' = 1$–4) and the calculation of Chung *et al*. for the band 5–0 in Fig. 2. The results are in good agreement with those presented by Ogilvie *et al*.[19] and Chung *et al*.[20] All results for the $\Delta = 1$–5 bands show that centrifugal distortion has only a minor influence on line intensities of the fundamental band but can be substantial in overtone transitions. The effect of centrifugal distortion on intensi-

ties increases with increasing $\Delta\upsilon$. The Herman–Wallis factor for the 5–0 transition has a qualitatively different shape from and a larger magnitude than that of the lower overtones. It also clearly indicates that the intensities of the 5–0 band in branch *P* are greater than those of the corresponding branch *R* lines. Chung *et al*. argued that several factors are responsible for such a condition, including the mutual interactions between higher-order terms of mechanical and electrical anharmonicities.[20] Although the Herman–Wallis factors of the bands 1–0, 2–0, and 3–0 calculated using the EDMF of Langhoff *et al*. agree with the measurements and calculations, the EDMFs of the bands 4–0 and 5–0, illustrated in Fig. 2 disagree with the experimental nor calculated results.[36] This indicates that the present *ab initio* calculated EDMF is relatively accurate and may be adequate to evaluate line intensities.

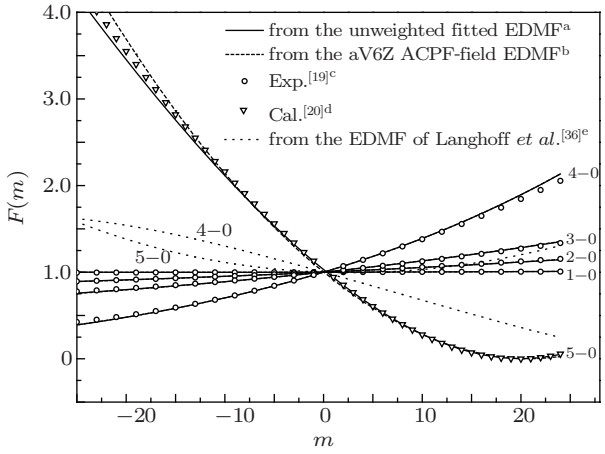


Fig. 2. Herman–Wallis factors: [a,b]for bands υ'–0 ($\upsilon' = 1$–5), [c]for bands υ'–0 ($\upsilon' = 1$–4), [d]for band 5–0, and [e]for bands 4–0 and 5–0.

3.4. Calculations and comparisons of line intensities

By combining the RKR potential, the EDMFs from the present weighted fits, and the aV6Z ACPF-field calculations, we calculate the rovibrational matrix moments that are used to compute the line intensities for the υ'–0 ($\upsilon' = 1$–5) bands, in units of cm/mol at 296 K. The line intensities are then compared with the most current HITRAN (2012) database and measurements of the fundamental band and overtone bands up to $\upsilon' = 5$.[2] The results of the comparisons are plotted in Figs. 3–7.

In Fig. 3, the calculated line intensities for the 1–0 band of CO ($X^1\Sigma^+$) are compared using measurements from Zou *et al.*[7] and the HITRAN database. The line intensities calculated using the present unweighted fitted EDMF are in better agreement with the experimental results of Zou *et al.*[7] than the intensities in HITRAN. At $-23 \leq m \leq 25$, the discrepancies in line intensities between the fitted EDMF and the experimental results of Zou *et al*. are estimated to be $-2.36\%\sim 2.65\%$, while the discrepancies from the HITRAN comparison with the experimental results range from -0.38% to -5.38%. The intensities in the HITRAN database are typically lower than the measurements given by Zou *et al*. The line intensities calculated using the aV6Z ACPF-field EDMF are somewhat larger than the ones of this fitted calculation, the HITRAN database, and Zou *et al*. Their discrepancies with the measurements are about $1.12\%\sim6.38\%$, which indicates that our *ab initio* results are also acceptable. For the 1–0 band, the band strengths calculated using the unweighted fitted and aV6Z ACPF-field EDMFs are 1.027×10^{-17} cm/mol and 1.061×10^{-17} cm/mol, respectively. These values agree well with the value of $1.022\pm0.036\times10^{-17}$ cm/mol derived by Varanasi and Sarangi and other data.[4,6,7,10]

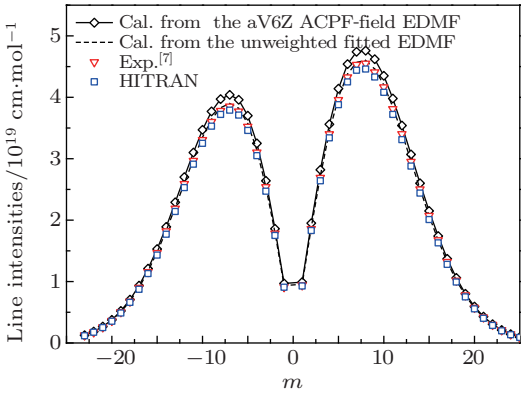


Fig. 3. (color online) Comparisons of the present calculated line intensities with the measurements and the HITRAN database for the band 1–0 of the CO.

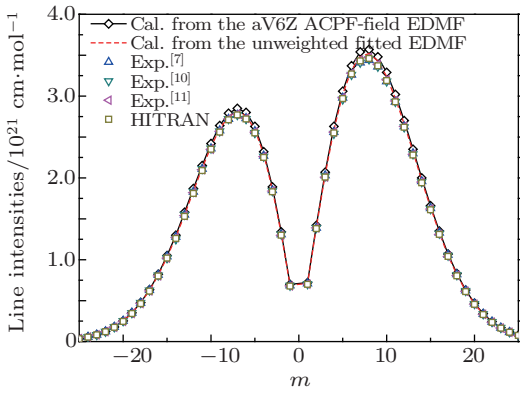


Fig. 4. (color online) Comparisons of the present calculated line intensities with the measurements and the HITRAN database for the band 2–0 of the CO.

Figure 4 illustrates the comparison for the 2–0 band. The results show that the line intensities of the unweighted fit agree well with the HITRAN database and the experimental line intensities of Zou *et al*. and Devi *et al*.[2,7,10,11] The line intensities from the aV6Z field EDMF are slightly larger than the measurements of Zou *et al*. and Devi *et al*.,[7,10,11] and their discrepancies are typically within $\pm3\%$. The band strengths that are obtained from the unweighted fitted and aV6Z ACPF-field EDMFs are 7.649×10^{-20} cm/mol and 7.768×10^{-20} cm/mol. Both agree well with the value of

$7.466\pm0.002\times10^{-20}$ cm/mol computed using a fitted vibrational matrix moment and the experimental value of $7.532\pm0.066\times10^{-20}$ cm/mol.[7,41]

The measurements for the 3–0 band given in Refs. [2], [13]–[15], and [17] are compared with the measurements made in this work and with those in the HITRAN database as shown in Fig. 5. The line intensities from the present study and HITRAN database[2] are consistent with the 3–0 band measurements presented in the literature. While the results of the unweighted fitted EDMFs and the aV6Z ACPF-field EDMFs are within 1% in agreement with the values provided by Chackerian *et al.*[15] and Sung *et al.*,[17] and the line intensities in the HITRAN [2] database correspond more closely to those of Henningsen *et al.*[13] and Picqué *et al.*[14]

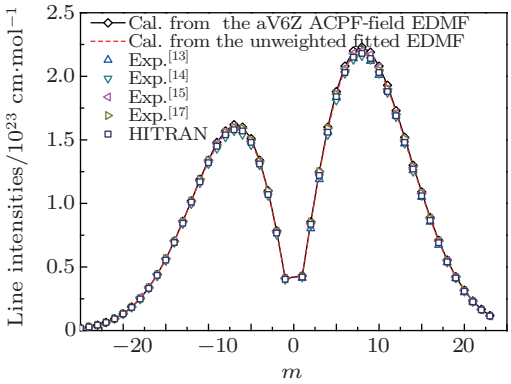


Fig. 5. (color online) Comparisons of the present calculated line intensities with the measurements and the HITRAN database for the band 3–0 of the CO.

Though Ogilvie *et al.* measured the strengths of lines for vibration–rotational bands of $^{12}C^{16}O$, including the 4–0 band, the parameters of the line intensities are not listed in their paper.[19] Therefore, only the early experimental data of Chackerian and Valero[18] are used for fits and comparison. These measurements as shown in Fig. 6, are compared with the calculated line intensities of the 4–0 band and the corresponding values in the HITRAN database.[2] The line intensities of the *P* and *R* branches as determined with the unweighted fit, are consistent with the referenced experimental results. Furthermore, the line intensities of the aV6Z field EDMF of the *P* branch are in better agreement with the experimental results than those of the *R* branch. In contrast, the line intensities from the HITRAN database match better with the measurements in the *R* branch.[2] However, the values from the unweighted fitted EDMF, the aV6Z ACPF-field EDMF, and HITRAN do not agree with the experimental results when considering the intensities of the *P*(15), *R*(20), and *R*(23) lines. The discrepancy of the *R*(23) line exceeds 20%, and it may arise from the large error of the measurement. Still, values from the two EDMFs and HITRAN[2] are consistent with each other.

The line intensity measurements for the 5–0 overtone band are only performed by Chung *et al.* who merely presented 16 lines of the *P* branch with an overly high reported uncertainty.[20] The minimum uncertainty of the line strength is likely to be 15%. The comparisons of line intensities for the 5–0 band appear in Fig. 7. There are rather large discrepancies between the measurements and calculations of Chung *et al.*, i.e., the line intensities of the unweighted fit and of the aV6Z ACPF-field EDMF.[20] The unweighted fit line intensities agree better with the results using the aV6Z ACPF-field EDMF. The calculated results again show that the line intensities in branch *P* are truly greater than those in branch *R*. For the 5–0 band, the band strengths obtained from the weighted fitted and aV6Z ACPF-field EDMFs are 5.585×10^{-27} cm/mol and 5.674×10^{-27} cm/mol, which are in close agreement with the experimental results of $5.1\pm1.3\times10^{-27}$ cm/mol.[20] Considering the rather large experimental uncertainties, we argue that the present intensities of the unweighted fitted line and the aV6Z ACPF-field EDMFs are still reliable and reflect the basic qualitative characteristics of spectral lines.

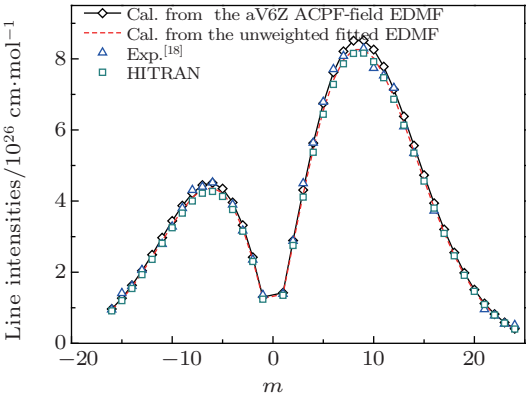


Fig. 6. (color online) Comparisons of the present calculated line intensities with the measurements and the HITRAN database for the band 4–0 of the CO.

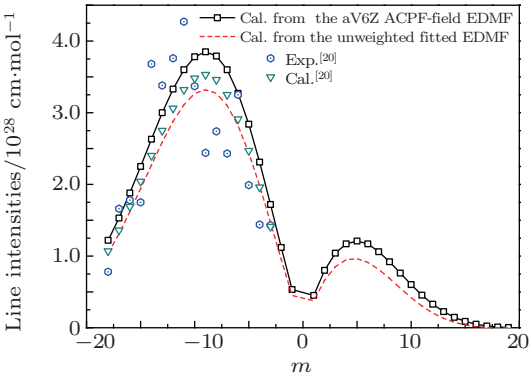


Fig. 7. (color online) Comparisons of the line intensities of the CO 5–0 band with the measurements and the calculations of Chung *et al.*[20]

The comparisons of line intensity, presented here, between the values from the HITRAN database and experimental measurements clearly show that the EDMF can be directly constructed from the experimental rovibrational transition matrix elements and can provide accurate values for CO ($X^1\Sigma^+$).

Although the line intensities calculated using the aV6Z ACPF-field EDMF are greater than the measurements at the υ'–0 ($\upsilon' = 1$–5) band, the discrepancies are within the admissible range of deviation between theoretical calculation and measurement.

4. Conclusions

By using a weighted and unweighted approach to fit the best available data of individual rovibrational transitions of CO ($X^1\Sigma^+$), we obtain an accurate EDMF within the valid range of 0.967 Å$\leq r \leq$1.322 Å, which agrees well with that of Chung *et al.*[20] Meanwhile, an accurate *ab initio* EDMF is also calculated at the ACPF/aug-cc-pV6Z level with a finite-field of ±0.005 a.u. The fitted EDMF in the valid range shows close agreement with the *ab initio* EDMF, and for small values of r, the electric dipole moment values are slightly smaller than the previous theoretical results of Langhoff and Bauschlicher.[36] Combining the RKR potential curve and these EDMFs, the transition matrix moments are computed and compared with the experimental ones. The vibrational transition matrix moments $\mu_{\upsilon',\upsilon''}$ calculated by using our unweighted fitted EDMF are in excellent agreement with the experimental values. The Herman–Wallis factors calculated using the present aV6Z ACPF-field EDMF also agree well with the experimental measurements. Comparisons are made among line intensities calculated here, reported in the HITRAN[2] database and obtained from experimental measurements. The results clearly show that the present unweighted fitted and aV6Z ACPF-field EDMFs are accurate and useful in predicting the spectral properties of the CO molecule.

References

[1] Winnewisser G, Herbst E and Ungerechts H 1992 *Spectroscopy of the Earth's atmosphere and interstellar mediu* (Boston: Academic Press)
[2] Rothman L S, Gordon I E, Babikov Y, Barbe A, Chris Benner D, Bernath P F, Birk M, Bizzocchi L, Boudon V, Brown L R, Campargue A, Chance K, Cohen E A, Coudert L H, Devi V M, Drouin B J, Fayt A, Flaud J M, Gamache R R, Harrison J J, Hartmann J M, Hill C, Hodges J T, Jacquemart D, Jolly A, Lamouroux J, LeRoy R J, Li G, Long D A, Lyulin O, Mackie C, Massie S T, Mikhailenko S, Müller H S, Naumenko O, Nikitin A, Orphal J, Perevalov V I, Perrin A, Polovtseva E R, Richard C, Smith M A H, Starikova E, Sung K, Tashkun S, Tennyson J, Toon G C, Tyuterev Vl G and Wagner G 2013 *J. Quantum Spectrosc. Radiat. Transfer* **130** 4
[3] Rothman L S, Gordon I E, Barberb R J, Dothe H, Gamache R R, Goldman A, Perevalov V I, Tashkun S A and Tennyson J 2010 *J. Quantum Spectrosc. Radiat. Transfer* **111** 2139
[4] Varansi P and Sarangi S 1975 *J. Quantum Spectrosc. Radiat. Transfer* **15** 473
[5] Varghese P L and Hanson R K 1980 *J.Quantum Spectrosc. Radiat. Transfer* **24** 479
[6] Chackerian Jr C, Guelachvili G and Tipping R H 1983 *J. Quantum Spectrosc. Radiat. Transfer* **30** 107
[7] Zou Q and Varanasi P 2002 *J. Quantum Spectrosc. Radiat. Transfer* **75** 63
[8] Bouanich J P and Brodbeck C 1974 *J. Quantum Spectrosc. Radiat. Transfer* **14** 1199
[9] Chandraiah G and Hébert G R 1981 *Can. J. Phys.* **59** 1367
[10] Devi V M, Benner D C, Smith M A H, Rinsland C P and Mantz A W 2002 *J. Quantum Spectrosc. Radiat. Transfer* **75** 455
[11] Devi V M, Benner D C, Smith M A H, Mantz A W, Sung K, Brown L R and Predoi-Cross A 2012 *J. Quantum Spectrosc. Radiat. Transfer* **113** 1013
[12] Toth R A, Hunt R H and Plyler E K 1969 *J. Mol. Spectrosc.* **32** 85
[13] Henningsen J, Simonsen H, M?gelberg T and Truds? E 1999 *J. Mol. Spectrosc.* **193** 354
[14] Picqué N, Guelachvili G, Dana V and Mandin J Y 2000 *J. Mol. Spectrosc.* **517–518** 427
[15] Chackerian C Jr, Freedman R, Giver L P and Brown L R 2001 *J. Mol. Spectrosc.* **210** 119
[16] Jacquemart D, Mandin J Y, Dana V, Picqué N and Guelachvili G 2001 *Eur. Phys. J. D* **14** 55
[17] Sung K and Varanasi P 2004 *J. Quantum Spectrosc. Radiat. Transfer* **83** 445
[18] Chackerian C Jr and Valero Francisco P J 1976 *J. Mol. Spectrosc.* **62** 338
[19] Ogilvie J F, Cheah S L, Lee Y P and Sauer S P A 2002 *Theor. Chem. Acc.* **108** 85
[20] Chung C Y, Ogilvie J F and Lee Y P 2005 *J. Phys. Chem. A* **109** 7854
[21] Chackerian C Jr 1976 *J. Chem. Phys.* **65** 4228
[22] Chackerian C Jr and Tipping R H 1983 *J. Mol.Spectrosc.* **99** 431
[23] Bouanich J P, Thanh N V and Rossi I 1983 *J. Quantum Spectrosc. Radiat. Transfer* **30** 9
[24] Chackerian C Jr, Fakkenq R, Guelachvili G, Rossetti C and Urba W 1984 *Can. J. Phys.* **62** 1579
[25] Kiriyama F and Rao B S 2000 *J. Quantum Spectrosc. Radiat. Transfer* **65** 673
[26] Buldakov M A and Cherepanov V N 2004 *J. Phys. B: At. Mol. Opt. Phys.* **37** 3973
[27] Goorvitch D, Chackerian C and JR 1994 *Astrophys. J. Suppl. Ser.* **91** 483
[28] Goorvitch D, Chackerian C and JR 1994 *Astrophys. J. Suppl. Ser.* **92** 311
[29] Goorvitch D 1994 *Astrophys. J. Suppl. Ser.* **95** 535
[30] Young L A and Eachus W J 1966 *J. Chem. Phys.* **44** 4195
[31] Werner H J 1981 *Mol. Phys.* **44** 111
[32] Cooper D M and anghoff S R 1981 *J. Chem. Phys.* **74** 1200
[33] Diercksen G H F and Sadlej A 1985 *Chem. Phys.* **96** 17
[34] Diercksen G H F and Sadlej A 1985 *Chem. Phys.* **96** 43
[35] Kellö V, Noga J, Dierchsen G H F and Sadlej A 1988 *Chem. Phys. Lett.* **152** 387
[36] Langhoff S R and Bauschlicher Jr C W 1995 *J. Chem. Phys.* **102** 5220
[37] Schautz F and Flad H J 1999 *J. Chem. Phys.* **110** 11700
[38] Tipping R H and Herman R M 1970 *J. Mol. Spectrosc.* **36** 404
[39] Kiriyama F, Rao B S and Nangia V K 2001 *J. Quantum Spectrosc. Radiat. Transfer* **69** 35
[40] Li G, Gordon I E, Bernath P F and Rothman L S 2011 *J. Quantum Spectrosc. Radiat. Transfer* **112** 1543
[41] Brault J W, Brown L R, Chackerian C Jr, Freedman R, Predoi-Cross A and Pin A S 2003 *J. Mol. Spectrosc.* **222** 220
[42] Knowles P J and Werner H J 1985 *Chem. Phys. Lett.* **115** 259
[43] Gdanitz R J and Ahlrichs R 1988 *Chem. Phys. Lett.* **143** 413
[44] Werner H J, Knowles P J, Knizia G, Manby F R, Schütz M *et al.* MOLPRO, version 2009.1, a package of *ab initio* programs, 2009, see http://www.molpro.net.
[45] Peterson K A, Woon D E and Dunning T H 1994 *J. Chem. Phys.* **100** 7410
[46] Peterson K A, Kendall R A and Dunning T H 1993 *J. Chem. Phys.* **99** 1930
[47] Dunning T H 1989 *J. Chem. Phys.* **90** 1007
[48] Le Roy R J April 2007 LEVEL 8.0, University of Waterloo Chemical Physics Research Report CP-663. see:<http://scienide2.uwaterloo.ca/∼rleroy/level/>.
[49] Le Roy R J, RKR1 2.0, University of Waterloo Chemical Physics Research Report CP-657R; 2004. see:<http://scienide2.uwaterloo.ca/∼rleroy/rkr/>.
[50] Velichko T I, Mikhailenko S N and Tashkun S A 2012 *J. Quantum Spectrosc. Radiat. Transfer* **113** 1643
[51] Le Roy R J *A Practical Guide to Least-Squares Fitted, University of Waterloo Chemical Physics Research Report CP-628*; 1997, see:</http://scienide2.uwaterloo.ca/∼rleroy/?tting/>
[52] Huber K P and Herzberg G 1979 *Constants of Diatomic Molecules* (New York: Van Nostrand Reinhold).
[53] Chackerian C, Kshirsagar R J, Giver L P and Brown L R 1999 *OSA Tech. Dig.* (1999 *Opt. Soc. Am.*) **22** 139